

# Estimating Fatigue Curves With the Random Fatigue-Limit Model

**Francis G. Pascual**

Department of Mathematics and  
Program in Statistics  
Washington State University  
Pullman, WA 99164-3113  
(jpascual@math.wsu.edu)

**William Q. Meeker**

Department of Statistics and  
Center for Nondestructive Evaluation  
Iowa State University  
Ames, IA 50011  
(wqmeeke@iastate.edu)

In a fatigue-limit model, units tested below the fatigue limit (also known as the threshold stress) theoretically will never fail. This article uses a random fatigue-limit model to describe (a) the dependence of fatigue life on the stress level, (b) the variation in fatigue life, and (c) the unit-to-unit variation in the fatigue limit. We fit the model to actual fatigue data sets by maximum likelihood methods and study the fits under different distributional assumptions. Small quantiles of the life distribution are often of interest to designers. Lower confidence bounds based on likelihood ratio methods are obtained for such quantiles. To assess the fits of the model, we construct diagnostic plots and perform goodness-of-fit tests and residual analyses.

KEY WORDS: Akaike information criterion; Fatigue data; Maximum likelihood methods; Probability (P-P) plots; Random fatigue limit; Right censoring.

## 1 INTRODUCTION

### 1.1 Background

The relationship between fatigue life of metal, ceramic, and composite materials and applied stress is an important input to design-for-reliability processes. This article suggests a practical model to describe the relationship between fatigue life and applied stress and provides and illustrates corresponding data-analysis methods. This work is motivated by the need to develop and present quantitative fatigue-life information used in the design of jet engines.

Fatigue data are often presented in the form of a median S-N curve, a log-log plot of cyclic stress or strain  $s$  versus the median fatigue life  $N$  which is expressed in cycles to failure. An extension of this concept is the  $p$  quantile S-N curves, also called S-N-P curves, a generalization that relates the  $p$ -quantile of fatigue life to the applied stress or strain. Thus, each curve represents a constant probability of failure  $p$ , as a function of  $s$ . We shall

use the .05 and .95 quantile S-N curves to illustrate the variability of fatigue life. Unless otherwise specified, the S-N curve in the literature generally refers to the median curve. We shall use the S-N curve as such.

Fatigue data on ferrous and titanium alloys indicate that experimental units tested below a particular stress level are unlikely to fail. This limiting stress level is called the “fatigue limit” or “endurance limit.” The S-N curve for these materials exhibits a strong curvature and an asymptotic behavior near the fatigue limit. Most nonferrous metals such as aluminum, copper, and magnesium appear not to have a fatigue limit. S-N curves for these materials gradually drop off and never become horizontal. Failure will occur eventually if units are tested or are in service long enough.

In the literature, there is no clear agreement on the meaning of the terms “fatigue limit” and “endurance limit.” For nonferrous materials, it is common practice to define the “fatigue strength” to be the stress level below which failure will not occur before an arbitrary large number of cycles (e.g.  $10^7$  or  $10^8$  cycles). Collins (1993) and Dieter (1976) defined fatigue strength as such and used the term “fatigue limit” to imply infinite life. On the other hand, to represent fatigue strength at a prescribed long but finite life, Nelson (1990) and Colangelo and Heiser (1974) used the term “endurance limit,” whereas others use the term “fatigue limit.” In this article, we will use the term “fatigue limit” to mean the stress below which an infinite or a specified large number of cycles can be sustained, whichever case is appropriate.

The existence of infinite-life fatigue limits is still a subject of debate. Proponents of fatigue limits argue that the fatigue limit can be interpreted as the minimum force or stress required to cause crack propagation. The randomness in the fatigue limit is due in part to the location, orientation, size, and number of cracks, which are random themselves. The range of stress that will not result in crack propagation is important to the classic safe-life design approach that is based on high-cycle fatigue and infinite life. Information on the fatigue limit can be used to design components that are intended to last indefinitely.

On the other hand, others suggest that all units under cyclic stress will eventually fail if they are cycled long enough. Because it is not feasible to run fatigue tests indefinitely, it is difficult, if not impossible, to obtain evidence to support the existence (or nonexistence) of fatigue limits.

Nonetheless even when fatigue limits do not really exist, the random fatigue-limit model presented here provides a useful empirical model to describe the life-stress curvature and nonconstant variability that are typically observed in fatigue data. Moreover, for most materials, empirical S-N curves are generally relatively flat in the high-cycle or long-life range. In these cases, as with other applications of empirical modeling, it is, of course, dangerous to extrapolate outside of the range of the data.

## 1.2 Related Work

Hirose (1993) used maximum likelihood (ML) methods to estimate the fatigue limit and the mean life of polyethylene terephthalate (PET) films (used in electrical insulation) at the service stress. He fitted a Weibull inverse power relationship that includes a fixed fatigue limit parameter. Nelson (1984) studied the fatigue life of a nickel-base superalloy and fitted fatigue curves with nonconstant standard deviation to data with censored observations

using ML methods. He fitted a quadratic relationship to describe the curvature in the plot of (log) fatigue life versus (log) pseudo-stress. Shen, Wirsching, and Cashman (1996a) reviewed previous work on statistical models that characterize fatigue strength and describe trends in fatigue data. They compared the fits of such models to several fatigue data sets. Pascual and Meeker (1997) presented a model with a fatigue limit parameter and nonconstant standard deviation of log fatigue life to describe curvature and nonconstant variance in stress-life relationships. They fit the model to the nickel-base superalloy data studied by Nelson (1984). They also studied the effect that test length has on precision of estimates by analyzing simulated datasets based on their model. Nelson (1990, pp. 93-95) suggested modeling the fatigue limit as a random parameter; that is, test specimens have different fatigue limits according to some distribution called the “strength distribution.” Dieter (1976) discussed the statistical (random) nature fatigue limits and mentioned that, in heat-treated alloy of forging steel, 95% of fatigue limits fall between 40,000 and 52,000 psi. Symonds (1996) gave typical approximate fatigue limits for different types of metal in reversed bending tests. Klesnil and Lukáš (1992, pp. 178-180) discussed the influence of grain size on the fatigue limit. Collins (1993, chap. 7) listed factors such as material composition, grain size and direction, heat treatment, and surface conditions that affect the S-N-P curves.

Little (1974) discussed the use of the up-and-down method to estimate the median fatigue limit with extreme value distributions based on ML and minimum chi-squared methods. The up-and-down method tests specimens in sequence at equally-spaced stress levels for a specified large number of cycles (e.g.,  $10^7$  cycles). A specimen is tested at the next lower (higher) stress level if the previous test produces a failure (right censored observation). Little (1990) presented a modified up-and-down test that uses a minimum variance strategy to choose the next stress level. The up-and-down method is an efficient and effective way of estimating the median fatigue limit. It is not used to estimate the stress-life relationship because the fatigue data are analyzed as quantal response data in which the main concern is whether or not a specimen on test has failed.

### 1.3 Overview

In Section 2, we discuss a statistical model for fatigue life that includes a random fatigue limit. This model describes and provides motivation for a fatigue life distribution that has the standard deviation as a function of stress. Section 3 describes ML methods. ML methods allow for censoring, which is common in fatigue testing, particularly at low levels of stress. Sections 4 and 5 illustrate the application of the model to actual fatigue data. We show how to compute ML estimates of parameters and fatigue-life distribution quantiles. Estimates of these quantiles are important inputs to product design processes and, thus, of most interest to engineers. Lower confidence bounds, based on likelihood ratio methods, are computed for these quantiles. We assess the fit of the model to the data by constructing diagnostic plots and performing goodness-of-fit tests and residual analyses. Section 6 outlines possible areas for further research.

## 2 THE RANDOM FATIGUE-LIMIT MODEL

There are two main considerations in modeling the relationship between the applied stress and fatigue life. First, often the standard deviation of fatigue life decreases as the applied stress increases. Second, curvature in fatigue curves suggests the inclusion of a fatigue limit in the statistical model for fatigue life. The random fatigue-limit model describes both of these characteristics.

Let  $Y$  be the fatigue life and  $s$  the stress level. We model  $Y$  as

$$\log(Y) = \beta_0 + \beta_1 \log(s - \gamma) + \epsilon, \quad s > \gamma,$$

where  $\beta_0$  and  $\beta_1$  are fatigue curve coefficients,  $\gamma$  is the fatigue limit of the specimen,  $\epsilon$  is the error term, and  $\log$  denotes natural logarithm. Let  $V = \log(\gamma)$ , and suppose that  $V$  has probability density function (pdf)

$$f_V(v; \mu_\gamma, \sigma_\gamma) = \frac{1}{\sigma_\gamma} \phi_V\left(\frac{v - \mu_\gamma}{\sigma_\gamma}\right)$$

with location and scale parameters  $\mu_\gamma$  and  $\sigma_\gamma$ , respectively.  $\phi_V(\cdot)$  is either the standardized smallest extreme value (sev) or normal pdf.

Let  $x = \log(s)$  and  $W = \log(Y)$ . Assume that, conditioned on a fixed value of  $V < x$ ,  $W|V$  has pdf

$$f_{W|V}(w; \beta_0, \beta_1, \sigma, x, v) = \frac{1}{\sigma} \phi_{W|V}\left(\frac{w - [\beta_0 + \beta_1 \log(\exp(x) - \exp(v))]}{\sigma}\right)$$

with location parameter  $\beta_0 + \beta_1 \log(\exp(x) - \exp(v))$  and scale parameter  $\sigma$ .  $\phi_{W|V}(\cdot)$  is either the standardized sev or normal pdf. The marginal pdf of  $W$  is given by

$$f_W(w; x, \boldsymbol{\theta}) = \int_{-\infty}^x \frac{1}{\sigma \sigma_\gamma} \phi_{W|V}\left(\frac{w - \mu(x, v, \boldsymbol{\theta})}{\sigma}\right) \phi_V\left(\frac{v - \mu_\gamma}{\sigma_\gamma}\right) dv,$$

where  $\boldsymbol{\theta} = (\beta_0, \beta_1, \sigma, \mu_\gamma, \sigma_\gamma)$  and  $\mu(x, v, \boldsymbol{\theta}) = \beta_0 + \beta_1 \log[\exp(x) - \exp(v)]$ . The marginal cumulative distribution function (cdf) of  $W$  is given by

$$F_W(w; x, \boldsymbol{\theta}) = \int_{-\infty}^x \frac{1}{\sigma_\gamma} \Phi_{W|V}\left(\frac{w - \mu(x, v, \boldsymbol{\theta})}{\sigma}\right) \phi_V\left(\frac{v - \mu_\gamma}{\sigma_\gamma}\right) dv,$$

where  $\Phi_{W|V}(\cdot)$  is the cdf of  $W|V$ . We will refer to this statistical model as the random fatigue-limit model. There are no closed forms for the density and distribution functions of  $W$ . They are, however, easy to evaluate numerically.

We will see that this model has the properties that one usually sees in fatigue-limit data. In particular, the model adequately describes curvature in the stress-life relationship and the increase in variability in log fatigue life at low stress/strain levels.

### 3 MAXIMUM LIKELIHOOD ESTIMATION

We use ML methods to estimate the parameters of the random fatigue-limit model. Statistical theory suggests that ML estimators, in general, have favorable asymptotic (large sample) properties. For “large” sample sizes and under certain conditions on the fatigue life distribution, the distribution of ML estimators is approximately multivariate normal with mean vector equal to the vector of true values being estimated and standard deviations no larger than that of any other competing estimators. See Nelson (1990, chap. 5) for an in-depth discussion of ML estimation with censored data.

Let  $y_p(s)$  be the  $p$  quantile of the life distribution at stress level  $s$ . We obtain ML estimates of  $y_p(s)$  for  $p = .05, .50$ , and  $.95$ . We compute approximate likelihood-ratio-based lower confidence bounds for the  $.01$  and  $.05$  quantiles of the life distribution. Ostrouchov and Meeker (1988) used Monte Carlo simulations to compare the accuracy of confidence intervals based on likelihood ratio and those based on asymptotic normal theory for interval-censored Weibull and lognormal data. Vander Wiel and Meeker (1990) did a similar study for a simple accelerated life-test model. Both articles concluded that likelihood confidence intervals have coverage probabilities generally closer to nominal confidence levels than those of normal approximation intervals even in small to moderate size samples.

#### 3.1 Parametric Likelihood

For the random fatigue-limit model defined previously with sample data  $w_1 = \log(y_1), \dots, w_n = \log(y_n)$  at log stress levels  $x_1, \dots, x_n$ , respectively, the likelihood is

$$L(\boldsymbol{\theta}) = \prod_{i=1}^n [f_W(w_i; x_i, \boldsymbol{\theta})]^{\delta_i} [1 - F_W(w_i; x_i, \boldsymbol{\theta})]^{1-\delta_i},$$

where

$$\delta_i = \begin{cases} 1 & \text{if } w_i \text{ is a failure} \\ 0 & \text{if } w_i \text{ is a censored observation.} \end{cases}$$

The function  $L(\boldsymbol{\theta})$  can be interpreted as being approximately proportional to the probability of observing  $y_1, \dots, y_n$  for a given set of parameters  $\boldsymbol{\theta}$ . Generally, it is easier to work with the log-likelihood function

$$\mathcal{L}(\boldsymbol{\theta}) = \log[L(\boldsymbol{\theta})] = \sum_{i=1}^n \mathcal{L}_i(\boldsymbol{\theta})$$

where

$$\mathcal{L}_i(\boldsymbol{\theta}) = \delta_i \log[f_W(w_i; x_i, \boldsymbol{\theta})] + (1 - \delta_i) \log[1 - F_W(w_i; x_i, \boldsymbol{\theta})]$$

is the contribution of the  $i$ th observation. The ML estimate  $\hat{\boldsymbol{\theta}}$  of  $\boldsymbol{\theta}$  is the set of parameter values that maximizes  $L(\boldsymbol{\theta})$  or  $\mathcal{L}(\boldsymbol{\theta})$ .

#### 3.2 Profile Likelihoods and Likelihood-Ratio-Based Confidence Regions

We use the profile likelihood to compute approximate confidence intervals for quantities or vectors of interest. These intervals are based on inverting a likelihood ratio test. Let

$\boldsymbol{\theta} = (\boldsymbol{\theta}_1, \boldsymbol{\theta}_2)$  be a partition of  $\boldsymbol{\theta}$  where  $\boldsymbol{\theta}_1$  is a vector of  $k$  quantities of interest. Let  $\hat{\boldsymbol{\theta}}$  denote the ML estimate of  $\boldsymbol{\theta}$ . The profile likelihood for  $\boldsymbol{\theta}_1$  is defined by

$$R(\boldsymbol{\theta}_1) = \max_{\boldsymbol{\theta}_2} \left[ \frac{L(\boldsymbol{\theta}_1, \boldsymbol{\theta}_2)}{L(\hat{\boldsymbol{\theta}})} \right].$$

A large value (close to 1) of  $R(\boldsymbol{\theta}_1)$  indicates that the observed data are highly probable for that value of  $\boldsymbol{\theta}_1$ , relative to the ML estimate. On the other hand, a small value (close to 0) of  $R(\boldsymbol{\theta}_1)$  indicates that the observed data are relatively unlikely for the given value of  $\boldsymbol{\theta}_1$ . When  $k = 1$ , plotting  $R(\boldsymbol{\theta}_1)$  against different values of  $\boldsymbol{\theta}_1$  yields a profile likelihood plot for  $\boldsymbol{\theta}_1$ .

When evaluated at the true value  $\boldsymbol{\theta}_1$ , the asymptotic distribution of  $-2 \log[R(\boldsymbol{\theta}_1)]$  is a chi-squared distribution with  $k$  df. As a result, an approximate  $100(1 - \alpha)\%$  confidence region for  $\boldsymbol{\theta}_1$  is given by the set of all  $\boldsymbol{\theta}_1$  such that

$$-2 \log[R(\boldsymbol{\theta}_1)] \leq \chi_{(k; 1-\alpha)}^2$$

or, equivalently,

$$R(\boldsymbol{\theta}_1) \geq \exp \left[ -\frac{\chi_{(k; 1-\alpha)}^2}{2} \right],$$

where  $\chi_{(k; 1-\alpha)}^2$  is the  $(1 - \alpha)$  quantile of a chi-square distribution with  $k$  df. If  $k = 1$ , the preceding inequalities yield confidence intervals. If  $k = 2$ , the equation

$$R(\boldsymbol{\theta}_1) = \exp \left[ -\frac{\chi_{(2; 1-\alpha)}^2}{2} \right]$$

defines a constant-likelihood contour line corresponding to a  $100(1 - \alpha)\%$  joint confidence region.

Confidence intervals based on the approximate normal distribution of studentized ML estimators can also be computed. As mentioned earlier, however, likelihood confidence intervals perform better in the sense that coverage probabilities are closer to nominal confidence levels than those of normal-approximation intervals.

## 4 LAMINATE PANEL DATA

In this section, we fit the random fatigue-limit model to fatigue data given by Shimokawa and Hamaguchi (1987). The data come from 125 specimens in four-point out-of-plane bending tests of carbon eight-harness-satin/epoxy laminate. Fiber fracture and final specimen fracture occurred simultaneously. Thus, fatigue life is defined to be the number of cycles until specimen fracture. The dataset includes 10 right-censored observations (known as “runouts” in the fatigue literature). Figure 1 shows the data and fitted random fatigue-limit models on a log-log scale with time on the horizontal axis, as is traditional in the fatigue literature. In this figure, “•” and “▷” represent failures and censored observations, respectively.

## 4.1 Maximum Likelihood Estimates of the Random Fatigue-Limit Model Parameters

We fit the random fatigue-limit model discussed in Section 2 to the data under the sev-sev, normal-normal, sev-normal, and normal-sev combinations for the respective distributions of  $V$  and  $W|V$ . Table 1 gives the ML estimates of the model parameters and the value of the log-likelihood for these estimates. The table includes ML estimates  $\hat{y}_{.05}(s)$  of the .05 quantile of fatigue life in units of thousands of cycles at stress levels  $s = 270, 280, 300, 340,$  and  $380$  MPa. We compute values of the Akaike information criterion (AIC) statistic for each model to identify which best approximates the true underlying model. The AIC statistic is given by

$$\text{AIC} = -2[\log_{\max} L(\boldsymbol{\theta}) - k],$$

where  $k$  is the number of model parameters. Smaller values of AIC indicate better fits. See Akaike (1973) for more details. Based on the AIC values, the normal-normal model ( $V$  and  $W|V$  are both normal) provides the best fit to the data among the four models. On the other hand, the sev-sev model gives the worst fit.

Table 1: *Maximum Likelihood Results for the Laminate Panel Data*

		Model			
		Sev-Sev	Normal-Normal	Sev-Normal	Normal-Sev
Loglikelihood	$\log[L(\boldsymbol{\theta})]$	-92.706	-86.221	-87.292	-87.603
AIC Statistic		195.412	182.442	184.584	185.206
Parameters	$\hat{\beta}_0$	35.575	30.272	33.025	29.435
	$\hat{\beta}_1$	-5.993	-5.100	-5.570	-4.950
	$\hat{\sigma}$	.239	.289	.141	.367
	$\hat{\mu}_\gamma$	5.295	5.366	5.323	5.390
	$\hat{\sigma}_\gamma$	.033	.031	.041	.020
Quantiles	$\hat{y}_{.05}(270)$	4443.0	6136.0	5530.0	6139.0
	$\hat{y}_{.05}(280)$	2319.0	2963.0	2810.0	2899.0
	$\hat{y}_{.05}(300)$	751.0	884.0	888.0	840.0
	$\hat{y}_{.05}(340)$	126.0	144.0	150.0	134.0
	$\hat{y}_{.05}(380)$	32.0	38.0	39.0	35.0

Figure 1 shows curves for the ML estimates of the .05, .50, and .95 quantiles of fatigue life under the different distribution combinations. When compared with the other combinations, the sev-sev combination consistently yields lower estimates of the .05 quantile and higher estimates of the .50 quantile of fatigue life. For the .95 quantile, all combinations yield similar estimates at the intermediate stress levels; the normal-sev combination yields higher estimates at the extreme stress levels. Comparing the fitted curves in these plots to the actual data suggests that the normal-normal and normal-sev models fit the data well.

Table 2 gives approximate confidence intervals for the normal-normal model parameters based on large-sample asymptotics and likelihood ratio methods for the laminate panel data. It also gives the asymptotic standard errors and coefficients of variation (the standard error as a percentage of the estimate) of the estimators. Note that the lower endpoint of the

likelihood ratio confidence interval for  $\sigma$  is 0. Both confidence intervals for  $\sigma_\gamma$  exclude 0. Thus, there is evidence suggesting the random nature of the fatigue limit. If the normal-normal model is appropriate, the estimated (log) fatigue-limit distribution is normal with mean 5.366 and standard deviation .031 log(MPa).

Table 2: *Confidence Intervals for the Parameters of the Normal-Normal Model for the Laminate Panel Data*

Parameter	Normal Approximation		Coefficient of Variation	Likelihood Ratio Confidence Interval
	Confidence Interval	Standard Error		
$\beta_0$	(21.948, 38.597)	4.247	14.04%	(23.809, 42.691)
$\beta_1$	(-6.577, -3.624)	.753	-14.76%	(-7.230, -3.927)
$\sigma$	(.128, .452)	.083	28.72%	(.000, .435)
$\mu_\gamma$	(5.235, 5.497)	.067	1.25%	(5.151, 5.462)
$\sigma_\gamma$	(.016, .047)	.008	25.48%	(.017, .053)

Figure 2 gives the profile likelihood plots for the model parameters for the laminate panel data. The plots indicate the approximate 95% likelihood-ratio-based confidence intervals for the parameters. These plots suggest that the likelihood has a unique maximum.

Viewing ML estimators as random variables, it is sometimes important or interesting to consider the propensity of these estimators to vary together. Issues involved in studying the correlation among parameter estimators are similar to issues of multicollinearity that arise in linear regression analysis. Two parameters with high correlation cannot be estimated independently and interpretation can be difficult. In severe cases, it may be that certain parameters are not identifiable and numerical problems (i.e., difficulty in finding the maximum of the likelihood) will arise. An estimate of the correlation matrix is often an output or an optional output of ML estimation. These correlation estimates are functions of the curvature of the likelihood, evaluated at its maximum (when one exists), as quantified by partial derivatives of the likelihood, evaluated at the ML estimates.

For a given model, the correlations among parameter estimators depend on the parameterization of the model and on the available data. As suggested by Ross (1990), some of numerical difficulties can be addressed by using a “stable” parameterization. Using a stable parameterization, if one is available, will also suggest what aspects of the model are easily identifiable. As with multicollinearity, identifiability can, in some circumstances, also be avoided by collecting appropriate data.

Table 3 gives the small-sample estimates of the correlations between parameter estimators for the laminate panel data. In this case, the estimators  $\hat{\beta}_0$ ,  $\hat{\beta}_1$ , and  $\hat{\mu}_\gamma$  are highly correlated with each other due in large part to the fact that these three parameters all strongly affected the position of the S-N curve. The high correlations could also be attributed to the lack of curvature in the S-N curve. A substantial amount of curvature is needed to precisely estimate these parameters. The high (negative) correlation between estimators  $\hat{\sigma}$  and  $\hat{\sigma}_\gamma$  suggests that the variability of fatigue life can be explained by either of the corresponding model parameters.

The contour plots for the model parameters reflect the correlations between parameter estimators. Narrower contours indicate higher correlations. Figures 3 and 4 give contour

Table 3: *Small-Sample Correlations between Model Parameter Estimates for the Laminate Panel Data*

	$\beta_0$	$\beta_1$	$\sigma$	$\mu_\gamma$	$\sigma_\gamma$
$\beta_0$	1.0000	-.9997	-.3100	-.9924	.6002
$\beta_1$		1.0000	.3117	.9892	-.5992
$\sigma$			1.0000	.3024	-.8152
$\mu_\gamma$				1.0000	-.6011
$\sigma_\gamma$					1.0000

plots for two pairs of parameters. The contour plots presented here indicate single peaks and, thus, the absence of multiple likelihood extrema.

## 4.2 Approximate 95% Lower Confidence Bounds for the .05 and .01 Quantiles of a Fatigue Life Distribution

Shen et al. (1996b) reviewed different methods of computing “design curves” that include quantile curves and tolerance limits for quantiles. In many applications, low quantiles of the life distribution are of primary interest. Using likelihood ratio methods we compute pointwise approximate 95% lower confidence bounds for the .05 and .01 quantiles of fatigue life based on the four distribution combinations discussed previously. Lower bounds for these quantities can be used to characterize fatigue strength. Figures 5 and 6 give plots of the lower confidence bounds for the .05 and .01 quantiles, respectively. In both plots, the sev-sev model gives the lowest confidence bounds. For the .05 quantile, the normal-normal, sev-normal, and normal-sev models give similar bounds. There are clearer differences among these three models for the .01 quantile. Here, the normal-normal model gives the highest bounds.

Figure 1 shows that, for the range of stress in the data, there is a one-to-one correspondence between the .05 quantile and the applied stress. In particular, the .05 quantile increases as stress is reduced. Thus, Figure 5 also provides approximate 95% upper confidence bounds for the stress level yielding a particular .05 quantile. To obtain these bounds graphically, we locate the point on the curve corresponding to the desired quantile value and read off the stress level on the vertical axis. A similar comment can be made about the .01 quantiles.

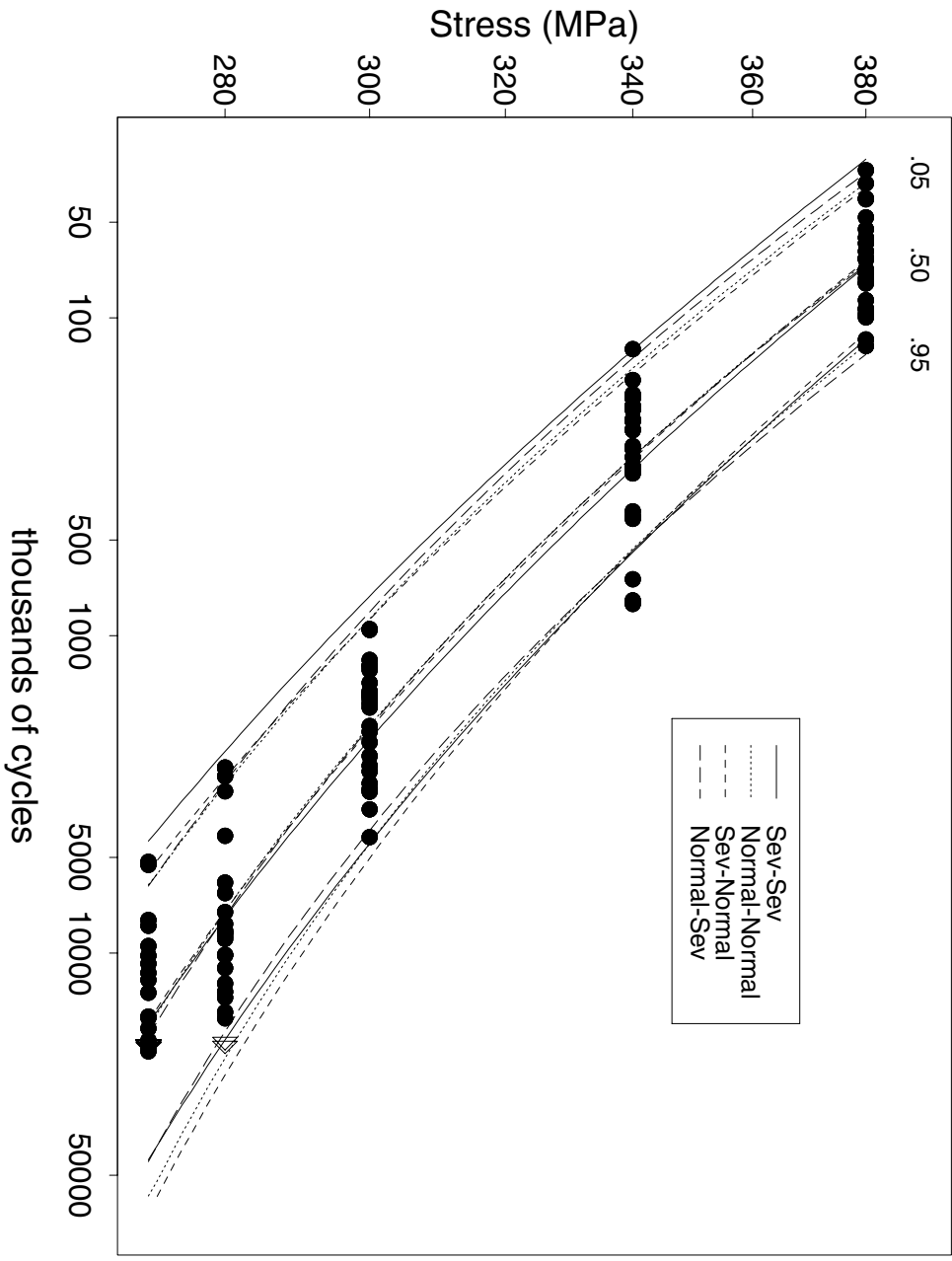


Figure 1: Log-Log S-N Plot for the Laminated Panel Data with ML Estimates of the .05, .50 and .95 Quantiles (● Failure, ◻ Censored Observation)

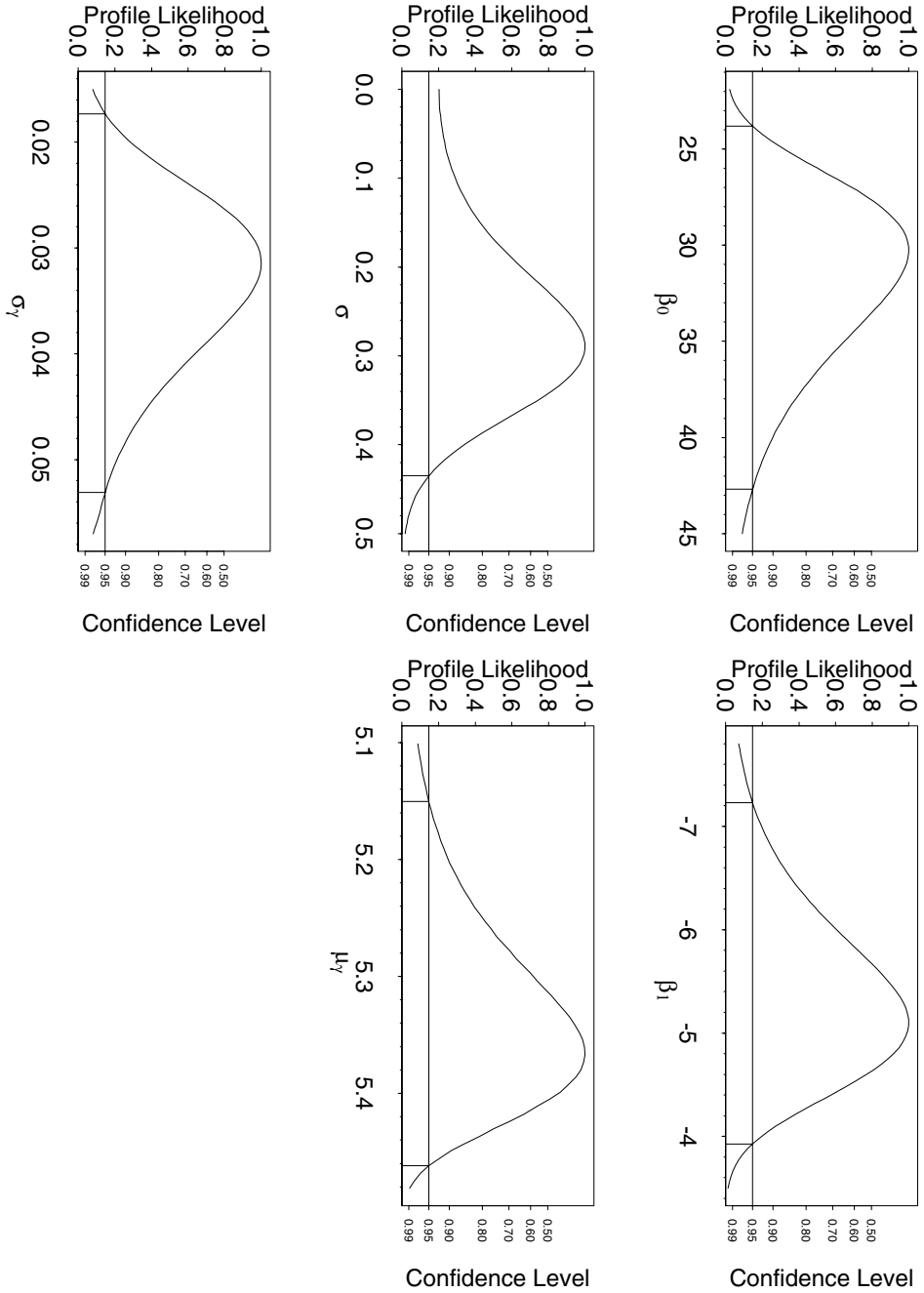


Figure 2: Profile Plots for Model Parameters for the Laminate Panel Data

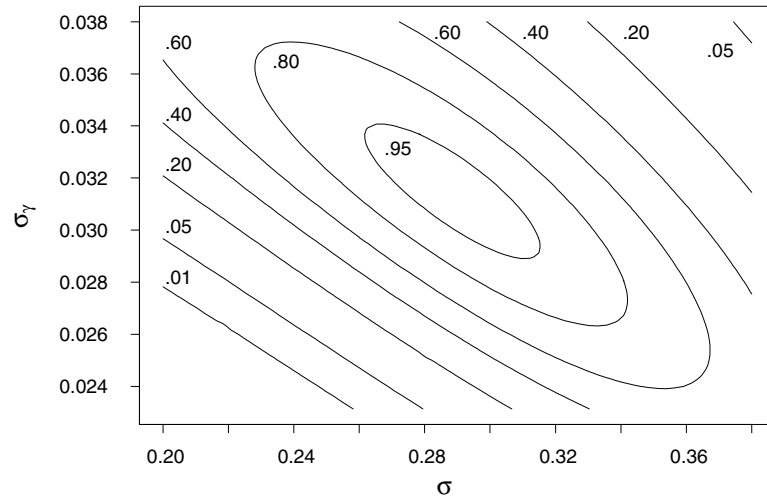


Figure 3: *Contour Plot for  $\sigma$  and  $\sigma_\gamma$  for the Laminate Panel Data*

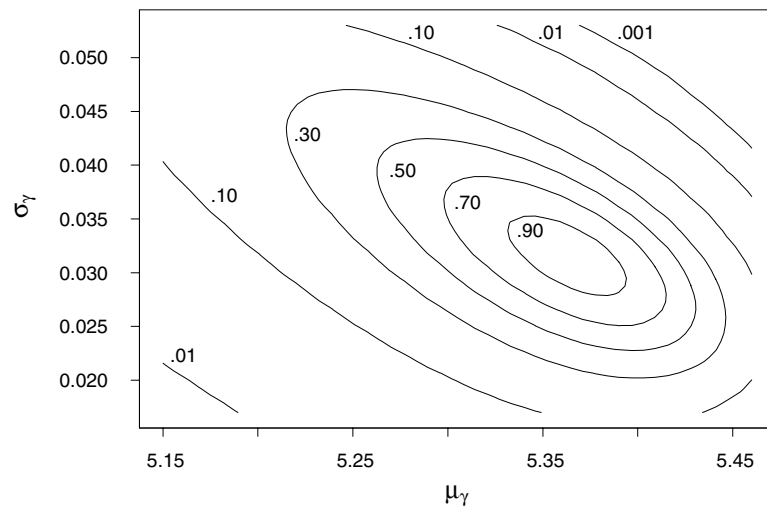


Figure 4: *Contour Plot for  $\mu_\gamma$  and  $\sigma_\gamma$  for the Laminate Panel Data*

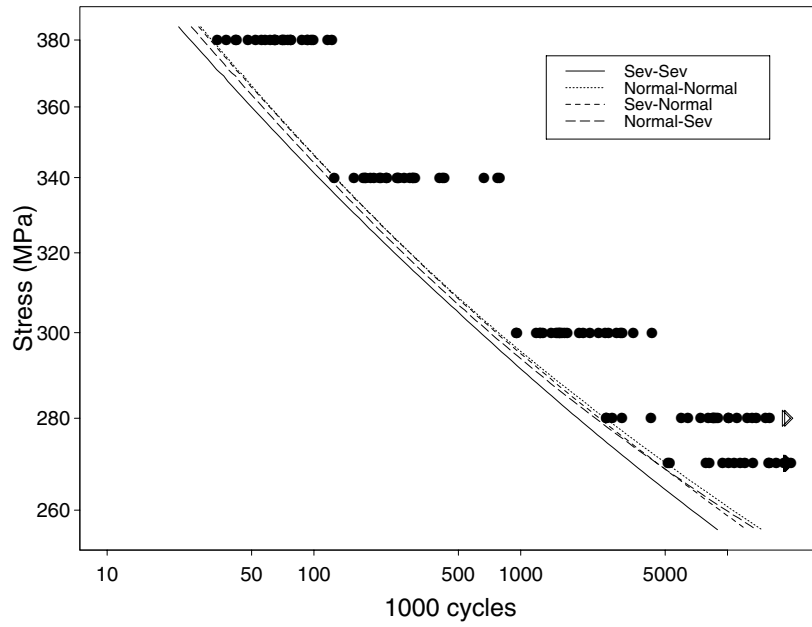


Figure 5: *Approximate 95% Lower Confidence Lower Bounds for the .05 Quantile of Fatigue Life for the Laminate Panel Data*

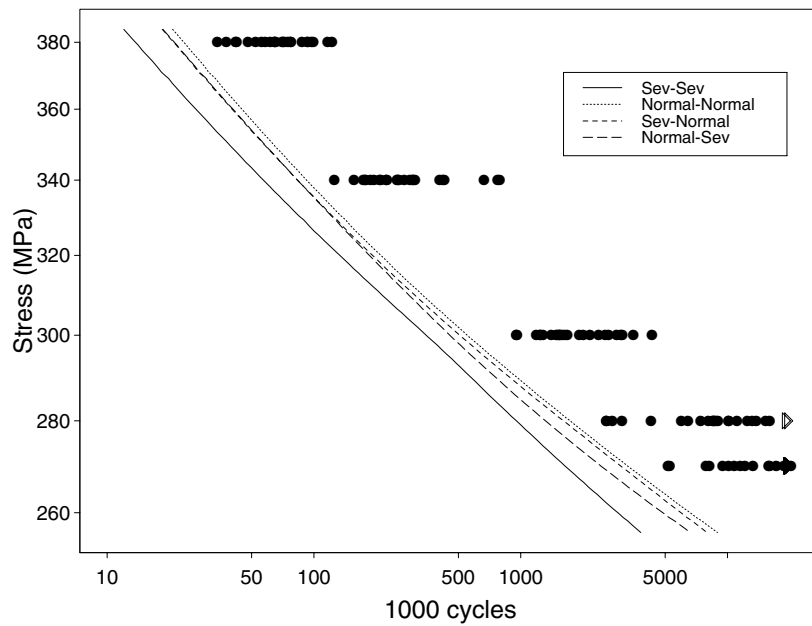


Figure 6: *Approximate 95% Lower Confidence Lower Bounds for the .01 Quantile of Fatigue Life for the Laminate Panel Data*

### 4.3 Probability (P-P) Plots

It is important to have a method for assessing distributional fit. A commonly used tool for comparing fits of competing distributions is the quantile-quantile (Q-Q) probability plot where the sample quantiles are plotted against the corresponding quantiles of a hypothesized distribution. We can use Q-Q plots to assess the fit of the distribution based on the ML estimates of model parameters. If a model is appropriate, the corresponding plot should be roughly linear. There are, however, several difficulties in using Q-Q plots. For instance, points in the distribution tails in Q-Q plots are those with the greatest variability. In general, these plots work well with location-scale distributions such as the normal, smallest extreme value and logistic distributions. For other distributions, like the random fatigue-limit model, separate Q-Q plots with different plotting axes are necessary for different parameter values, making it more difficult to display and compare the plots across different distribution combinations. Probability (P-P) plots provide a convenient alternative for this application. See Crowder, Kimber, Smith, and Sweeting (1991, chaps. 2 and 3) for more information on P-P plots.

For the random fatigue-limit model, the plotting points of a Q-Q or P-P plot are based on the Kaplan-Meier estimate of the survival probability and the ML estimate of the fatigue life distribution. Let  $y_1 \leq \dots \leq y_n$  be the ordered observations at log stress  $x$ . Let  $d_i$  be the number of failures at time  $y_i$  and  $n_i$  be the total number of unfailed and uncensored observations just prior to  $y_i$ . The Kaplan-Meier estimate of the survival probability  $S(y) = \Pr(Y \geq y)$  is given by

$$\hat{S}(y) = \prod_{\{i: y_i < y\}} \left(1 - \frac{d_i}{n_i}\right).$$

Suppose that failures occur at distinct times  $y'_1 < \dots < y'_r$ , where  $r \leq n$ . Let

$$p_i = 1 - \frac{1}{2} \{ \hat{S}(y'_i) + \hat{S}(y'_{i+1}) \}$$

for  $i = 1, \dots, r$ .

Let  $\hat{\theta}$  be the ML estimate of  $\theta$ . The plotting points of a Q-Q plot are given by

$$(\log(y'_i), F_W^{-1}(p_i; x, \hat{\theta}))$$

for  $i = 1, \dots, r$ . In practice, if the parent distribution  $F_W$  is location-scale, the location parameter is set to 0 and the scale parameter to 1. The plotting points of a P-P plot are given by

$$(p_i, F_W(\log(y'_i); x, \hat{\theta}))$$

for  $i = 1, \dots, r$ . Wilk and Gnanadesikan (1968) remarked that P-P plots are sensitive to discrepancies in the center of the distribution. In contrast to Q-Q plots, the extreme tail points in P-P plots have lower variability than those in the center. Michael (1983) suggested constructing a stabilized probability (S-P) plot with points,

$$\left( \frac{2}{\pi} \sin^{-1}(p_i), \frac{2}{\pi} \sin^{-1} \left[ F_W(\log(y'_i); x, \hat{\theta}) \right] \right),$$

to stabilize the variation in plotting points.

We feel that no particular method (P-P, Q-Q, or S-P plot) has any big advantage over the others for any particular part of the distribution. To know what can be expected from statistical noise, one only needs a method of calibration. In Crowder et al. (1991, p. 66) suggested using Monte Carlo methods to aid in the interpretation of P-P and Q-Q plots. They also provided pertinent references.

The axes for the P-P plots are the same for any set of parameter values. This facilitates comparison of P-P plots under competing models. Figure 7 gives P-P plots by stress level for the panel data. Linearity in the plots indicates a good fit. A careful inspection of the plots reveals that the sev-sev combination does not fit as well as the rest, particularly for stress levels 300 and 340 MPa. It appears that the normal-normal model has the best fit. The plots indicate a possible anomaly in stress levels 280 and 300 MPa. There are concentrations of points around 8.5 million cycles for 280 MPa and around 1.5 million cycles for 300 MPa. The Q-Q and S-P plots (not shown here) for the data yield similar information. The Q-Q, P-P, and S-P plots agree with the AIC statistics in Table 1 that the sev-sev and normal-normal models provide, respectively, the worst and best fits to the data.

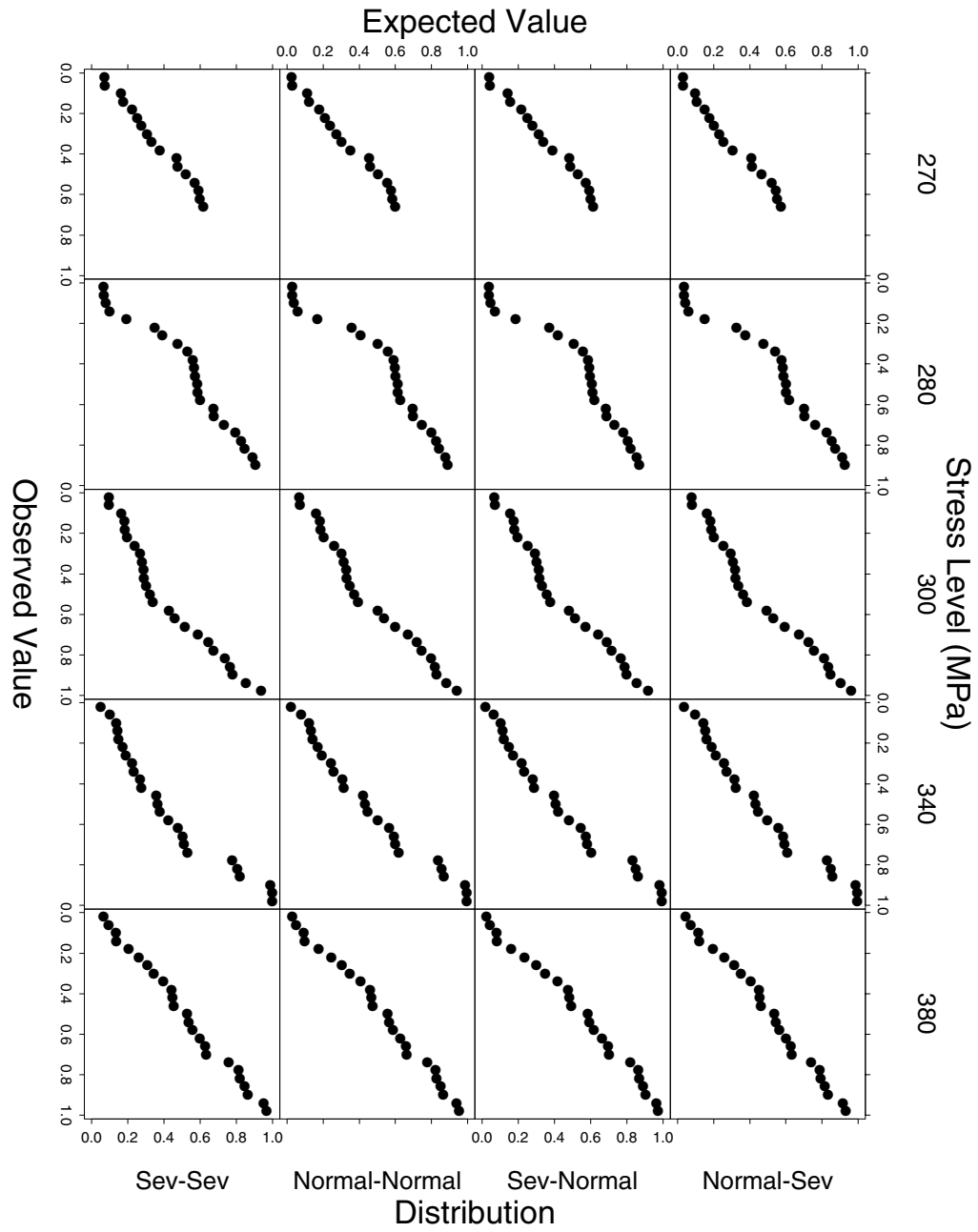


Figure 7: P-P Plots for the Laminate Panel Data

#### 4.4 Goodness-of-Fit Tests

We assess the statistical significance of departures from the random fatigue-limit model by performing empirical distribution function goodness-of-fit tests. We use Kolmogorov-Smirnov  $D$  statistics to perform these tests. For each stress level and distribution combination, we test the null hypothesis that the data obtained come from the corresponding random fatigue-limit distribution. To do this, we adapt the methods discussed by D'Agostino and Stephens (1986, chap. 4). Let  $w_1 = \log(y_1) \leq \dots \leq w_n = \log(y_n)$  be the ordered observations at log stress  $x$ . Let  $z_i = F_W(w_i; x, \boldsymbol{\theta})$  for  $i = 1, \dots, n$ . Under the true value  $\boldsymbol{\theta}$ ,  $Z_i = F_W(W_i; x, \boldsymbol{\theta})$  are ordered uniform random variables. If one or more components of  $\boldsymbol{\theta}$  are unknown, these components are replaced by estimates, for example, the ML estimate  $\hat{\boldsymbol{\theta}}$ . However,  $z_i = F_W(w_i; x, \hat{\boldsymbol{\theta}})$  will not be an ordered uniform sample even when the null hypothesis is true. D'Agostino and Stephens (1986) suggested modifications of the test statistic to account for the use of  $\hat{\boldsymbol{\theta}}$  in place of  $\boldsymbol{\theta}$ . The modifications are functions of the test statistic and sample size. They give tables of percentage points for the modified test statistic. We shall replace unknown parameter values with ML estimates and compute modified K-S test statistic values.

For complete (no censoring) datasets, the K-S  $D$  statistic is given by

$$D = \max_{1 \leq i \leq n} \left\{ \frac{i}{n} - z_i, z_i - \frac{i-1}{n} \right\}.$$

The statistic is modified using the formula

$$D^* = D(\sqrt{n} + .12 + \frac{.11}{\sqrt{n}}).$$

From D'Agostino and Stephens (1986, p. 105, Table 4.2), the reject region for the .05 level of significance is  $\{D^* > 1.358\}$ .

Suppose that the dataset contains  $r$  failures and  $n - r$  Type I censored observations that have log failure times above  $w_t$ . Let  $z_t = F_W(w_t; x, \hat{\boldsymbol{\theta}})$ . The K-S statistic adapted for Type I censoring is given by

$$D = \max_{1 \leq i \leq r} \left\{ \frac{i}{n} - z_i, z_i - \frac{i-1}{n}, z_t - \frac{r}{n} \right\}.$$

When unknown parameters are replaced by estimators, D'Agostino and Stephens (1986) suggested the modification

$$D^* = \sqrt{n}D + \frac{.19}{\sqrt{n}}.$$

The percentage points for  $D^*$  were given by D'Agostino and Stephens (1986, p. 112, Table 4.4).

In the laminate panel data, there are  $n = 25$  observations at each stress level. There are  $r = 8$  and 2 censored observations at stress levels 270 and 280 MPa, respectively. In both cases, we choose  $w_t = \log(20 \text{ million cycles})$  and compute modified K-S statistic for Type I censoring. At stress levels 300, 340 and 380 MPa all test units failed and, for these, we compute the modified K-S statistic for complete data.

Table 4 gives the test statistic values for each stress level. None of the tests are significant at the .05 level of significance. Thus, there is not enough evidence to rule out any of these distributions. The observed departures from linearity in the P-P plots may be explained by variability under the hypothesized models.

Table 4: *Kolmogorov-Smirnov D Statistic Values for the Fits of the Random Fatigue-Limit Models to the Laminate Panel Data*

Stress (MPa)	Sev-Sev	Normal-Normal	Sev-Normal	Normal-Sev
270	.4	.4	.5	.6
280	1.1	1.2	1.2	1.1
300	1.1	.9	.9	.9
340	1.2	.7	.8	.8
380	.4	.3	.4	.4

#### 4.5 Residual Analysis

To assess the validity of models and, in particular, detect problems with the life/stress relationship part of the models, we can study plots of residuals versus the stress levels. We follow methods suggested by Nelson (1973) to perform residual analysis on the fit of the normal-normal model. Figure 8 gives a plot of the fit of this model to the data. The plot includes density curves at selected stress levels.

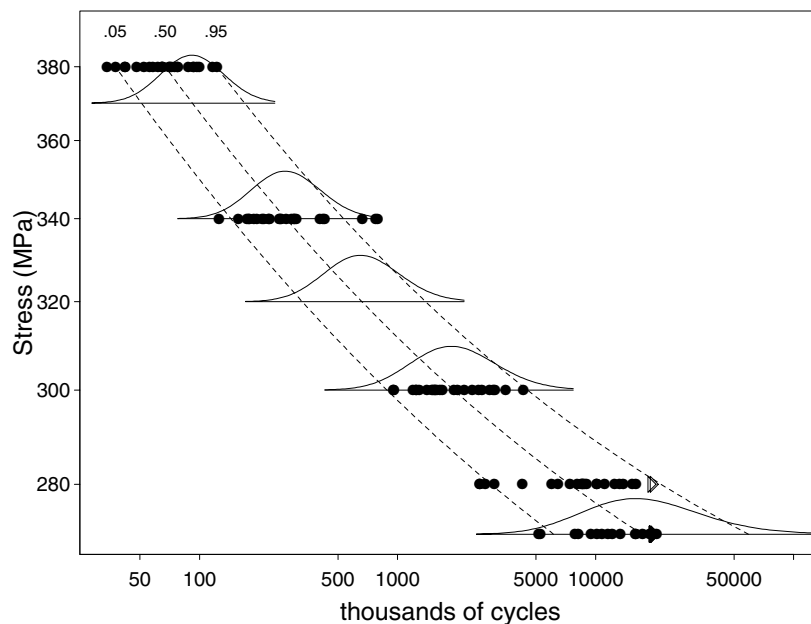


Figure 8: *Log-Log S-N Plot for the Laminate Panel Data with ML Estimates of Density Curves and the .05, .50, .95 Quantile Estimates under the Fitted Normal-Normal Model*

For the log stress level  $x_i$ , define the raw residual  $e_i$  by

$$e_i \equiv \log(y_i) - \hat{\mu}(x_i),$$

where  $\hat{\mu}(x_i)$  is the ML estimate of the mean log fatigue life at log stress level  $x_i$  conditioned on the specimen failing, that is, conditioned on the fatigue limit falling below the stress level. Because the standard deviation  $\sigma(x_i)$  of fatigue life varies with the log stress  $x_i$ , we define standardized residuals

$$e_i^* \equiv \frac{e_i}{\hat{\sigma}(x_i)}$$

where  $\hat{\sigma}(x_i)$  is ML estimate of the standard deviation of log fatigue life at log stress level  $x_i$  given that the specimen is going to fail. We use standardized residuals in the plots and refer to them as residuals henceforth.

The plots of residuals versus the stress levels should appear patternless. Figure 9 gives the plot of the residuals versus the stress levels for the normal-normal model. The plot does not show any clear patterns in the residuals.

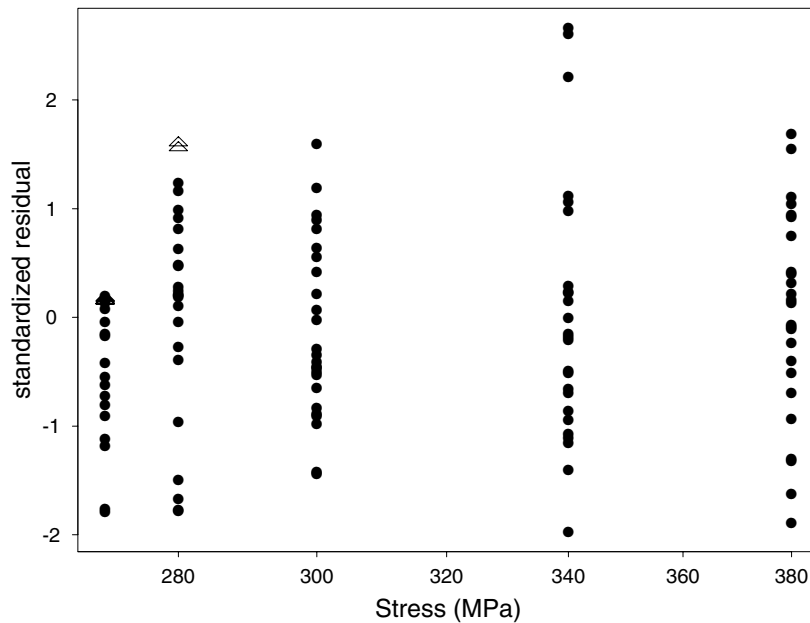


Figure 9: *Plot of Standardized Residuals versus Stress Levels for the Normal-Normal Model Fit to the Laminate Panel Data*

## 5 NICKEL-BASE SUPERALLOY DATA

In this section, we fit the random fatigue-limit model to a nickel-base superalloy fatigue dataset given by Shen (1994). The original dataset consists of 246 observations with 4 runouts. We fitted the model to the whole dataset and observed that the model did not

fit the data well in the low-strain region. One possible explanation for this is that the character of the failure mechanisms could be different at high strain levels. We refitted the model to the 115 observations for which strain is below .007 units. This improved the fit for the lower strain levels, implying that the omitted high-strain observations were influential, biasing estimates of fatigue life at low levels of strain.

Figure 10 gives a plot of the reduced dataset on a log-log scale. In this plot, “•” and “>” represent failures and censored observations, respectively. The applied force here is in strain units for which there are 32 unique values in contrast to 5 levels of stress in the laminate panel data. To assess the fits of the models to the data, we again construct P-P plots to compare combinations of distributions for  $W|V$  and  $V$ , and we perform residual analysis.

### 5.1 Maximum Likelihood Estimates of the Random Fatigue-Limit Model Parameters

Table 5 gives the ML estimates of the model parameters and the values of the log-likelihood under the ML estimates. The table includes AIC values and ML estimates  $\hat{y}_{.05}(s)$  of the .05 quantiles at strain levels  $s = 3.5, 4, 5, 6$ , and 7 for each model. The quantile estimates are in units of thousands of cycles. As in the previous example, the AIC values indicate that the normal-normal and the sev-sev combinations provide, respectively, the best and worst fit to the data.

Table 5: *Maximum Likelihood Results for the Nickel-Base Superalloy Data*

		Model			
		Sev-Sev	Normal-Normal	Sev-Normal	Normal-Sev
Loglikelihood	$\log[L(\boldsymbol{\theta})]$	-67.895	-62.082	-66.352	-63.161
AIC Statistic		145.790	134.164	142.704	136.322
Parameters	$\beta_0$	4.552	4.370	4.705	4.387
	$\beta_1$	-.923	-.928	-1.105	-.938
	$\sigma$	.227	.315	.203	.305
	$\mu_\gamma$	1.324	1.309	1.257	1.329
	$\sigma_\gamma$	.052	.044	.089	.046
Quantiles	$\hat{y}_{.05}(3.5)$	226.0	1131.8	219.9	354.3
	$\hat{y}_{.05}(4)$	82.8	110.2	90.0	96.8
	$\hat{y}_{.05}(5)$	30.7	36.0	36.2	36.0
	$\hat{y}_{.05}(6)$	18.8	21.6	21.5	21.8
	$\hat{y}_{.05}(7)$	13.6	15.5	15.0	15.7

Figure 10 shows curves for the ML estimates of the .05, .50, and .95 quantiles of fatigue life under the different distribution combinations. The models give similar estimates of the .50 and .95 quantiles. At the lower strain levels, the sev-sev model gives lower estimates of the .05 quantile, whereas the normal-normal model gives higher estimates.

The plot of the data in Figure 10 indicates that the standard deviation of fatigue life decreases with increasing strain. Even though the standard deviation is not written ex-

plicity as a function of the strain, the random fatigue-limit model describes the increased variability at lower levels of strain. Although not as obvious, a similar observation can be made for the laminate panel example in Section 4.

Table 6 gives approximate confidence intervals for normal-normal model parameters based on large-sample asymptotics and likelihood ratio methods. It also gives the asymptotic standard errors and coefficient of variation of the estimators. In contrast to the laminate panel results, the coefficients of variation are lower and the confidence intervals for  $\sigma$  do not contain 0. If the normal-normal model is appropriate, the estimated (log) fatigue-limit distribution is normal with mean 1.309 and standard deviation .044  $\log(1,000 \times \text{strain units})$ . Figure 11 gives the profile likelihood plots for the model parameters for the superalloy data. The profile likelihood plots and contour plots (not shown here) suggest that the likelihood has a unique maximum.

Table 6: *Confidence Intervals for the Parameters of the Normal-Normal Model for the Nickel-Base Superalloy Data*

Parameter	Normal Approximation		Coefficient of Variation	Likelihood Ratio
	Confidence Interval	Standard Error		Confidence Interval
$\beta_0$	(4.2018, 4.5375)	.0857	1.55%	(4.2334, 4.5809)
$\beta_1$	(-1.0938, -.7625)	.0845	-4.73%	(-1.1266, -.7810)
$\sigma$	(.2620, .3688)	.0273	11.87%	(.2651, .3740)
$\mu_\gamma$	(1.2751, 1.3424)	.0172	1.58%	(1.2626, 1.3374)
$\sigma_\gamma$	(.0247, .0637)	.0099	7.07%	(.0292, .0708)

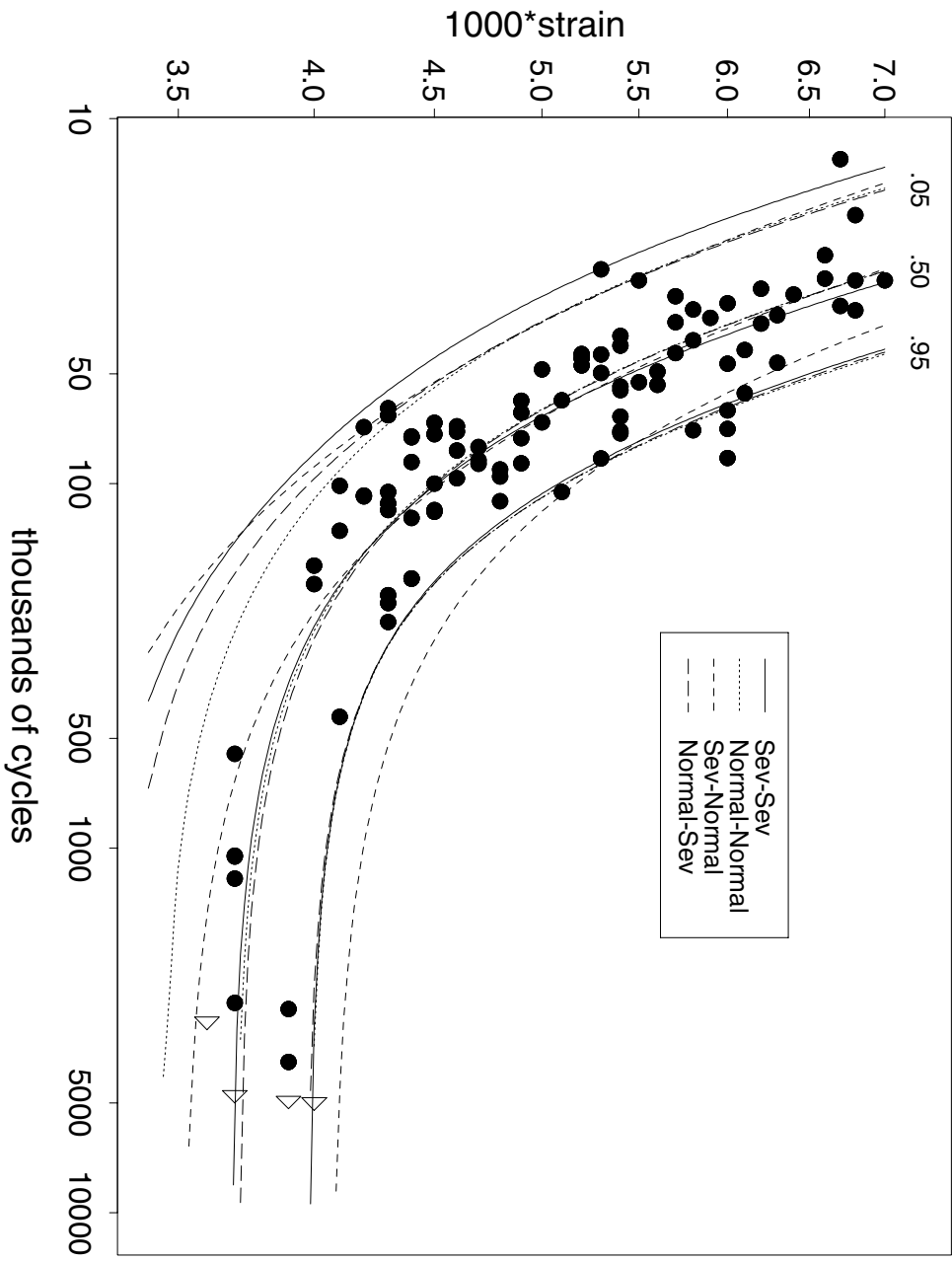


Figure 10: Log-Log S-N Plot for the Nickel-Base Superalloy Data with ML Estimates of the .05, .50 and .95 Quantiles (● Failure, ▷ Censored Observation)

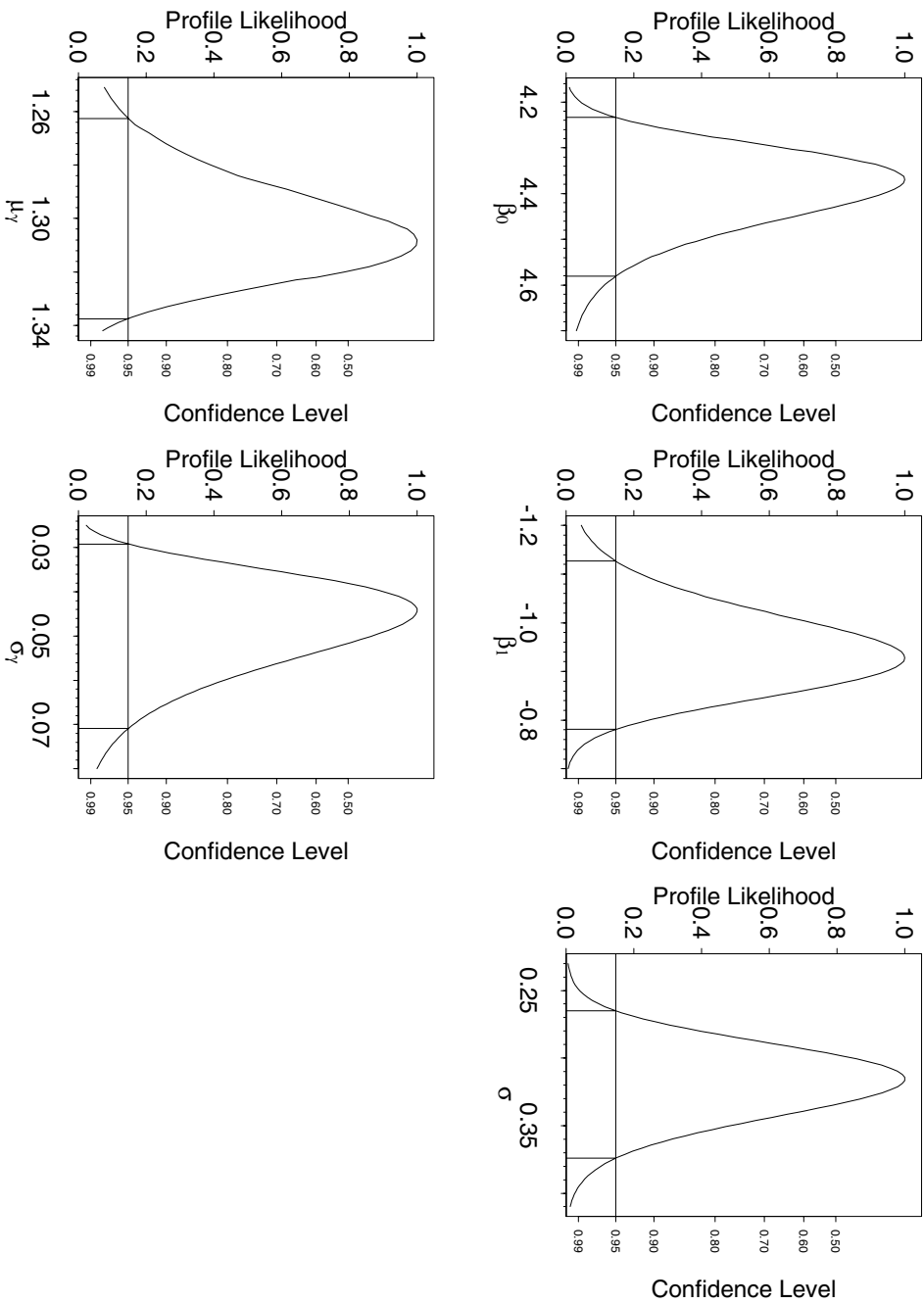


Figure 11: Profile Plots for Model Parameters for the Nickel-Base Superalloy Data

Table 7 gives the small-sample estimates of the correlations between parameter estimators for the nickel-base superalloy data. In contrast to the laminate panel results, the estimators  $\hat{\beta}_0$ ,  $\hat{\beta}_1$ , and  $\hat{\mu}_\gamma$  are not as highly correlated. Observe that there is substantial curvature in the superalloy S-N plot at the lower stress/strain levels unlike in the laminate panel S-N plot. Having a significant curvature in the empirical S-N plot improves the ability to estimate certain functions of the parameters. Thus, test runs should be conducted in a range of stress or strain that will produce a clear curvature in the S-N plot of the resulting data.

We constructed contour plots (not included here) for different pairs of parameter estimators. The plots reflect the correlations as given in Table 7. As in the previous example, the contour plots do not suggest possible multiple likelihood extrema.

Table 7: *Small-Sample Correlations between Model Parameter Estimates for the Nickel-Base Superalloy Data*

	$\beta_0$	$\beta_1$	$\sigma$	$\mu_\gamma$	$\sigma_\gamma$
$\beta_0$	1.0000	-.8060	-.1245	-.8657	.4892
$\beta_1$		1.0000	.1137	.7085	-.4184
$\sigma$			1.0000	.1511	-.3266
$\mu_\gamma$				1.0000	-.5416
$\sigma_\gamma$					1.0000

Because the superalloy data are not grouped by levels of stress or strain, we cannot construct P-P plots by strain levels. Instead, we take the following approach. Let  $W_i$  be the log fatigue life at log strain level  $x_i$  [i.e.,  $W_i = \log(Y_i)$ , for  $i = 1, \dots, n$ , where  $n$  is the sample size]. If  $F_W(W_i; x_i, \boldsymbol{\theta})$  is the true distribution of  $W_i$ , then  $Z_1 = F_W(W_1; x_1, \boldsymbol{\theta}), \dots, Z_n = F_W(W_n; x_n, \boldsymbol{\theta})$  are independently and identically distributed UNIF(0,1). Using this result, we construct P-P plots to assess whether if  $z_1 = F_W(w_1; x_1, \boldsymbol{\theta}), \dots, z_n = F_W(w_n; x_n, \boldsymbol{\theta})$  agrees with what we would expect to see from a random sample from a uniform distribution. See Figure 12. The plots show that the normal-normal and normal-sev models provide better fits than the other two distribution combinations. The S-P plots for the data yield similar information. The P-P and S-P plots agree with the AIC statistics in Table 5 that the normal-normal and normal-sev models provide the best fits.

Figures 13 and 14 give plots of the lower confidence bounds for the .05 and .01 quantiles, respectively. For either quantile, the normal-normal model gives wider confidence intervals than the other models, and, the sev-sev model gives narrower confidence intervals than the other models. At the lower strain levels, there are similarities between the sev-sev and sev-normal models and between the normal-normal and normal-sev models. At the higher strain levels, however, there are similarities between the sev-sev and normal-sev and between normal-normal and sev-normal.

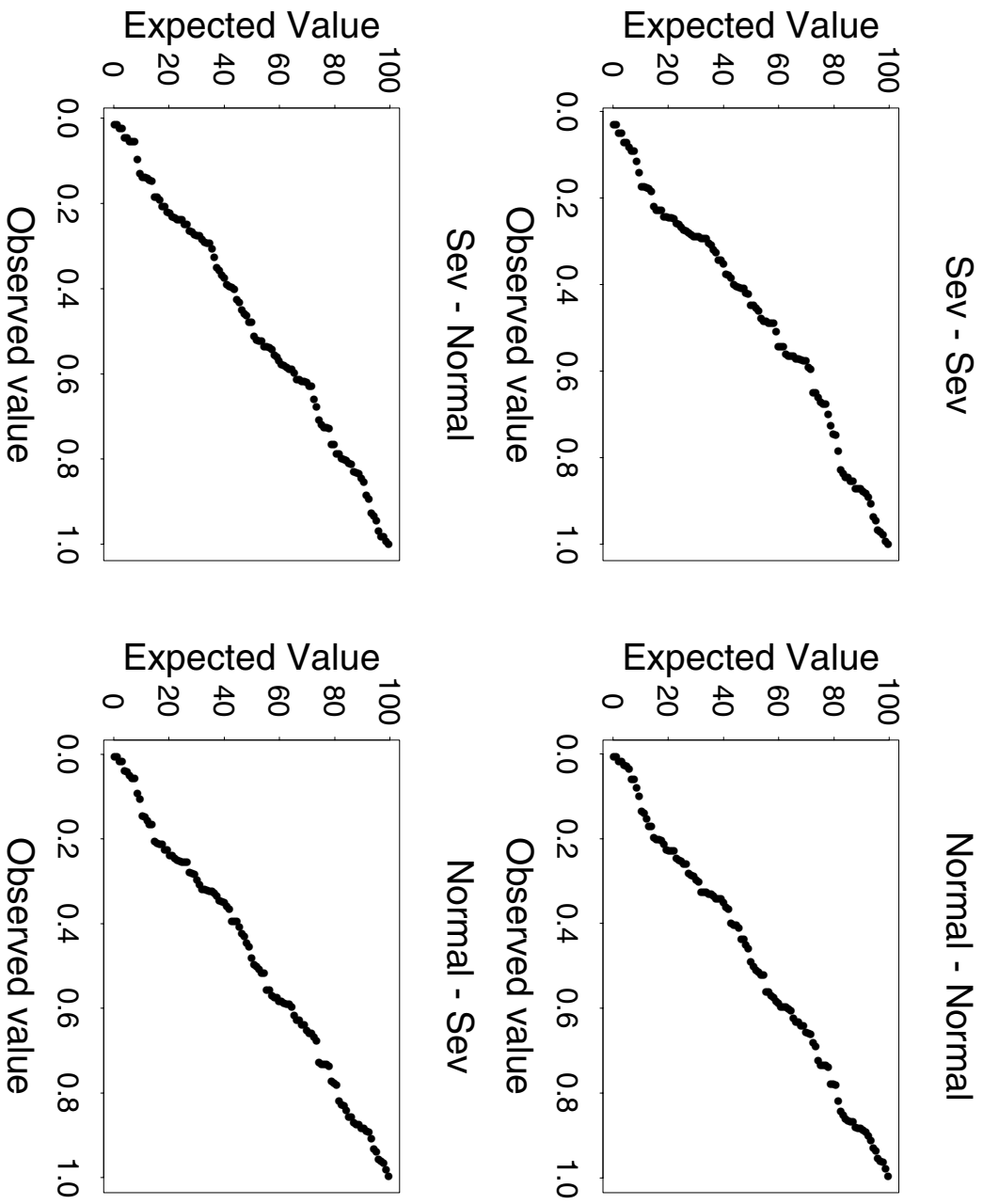


Figure 12: P-P Plots for the Nickel-Base Superalloy Data

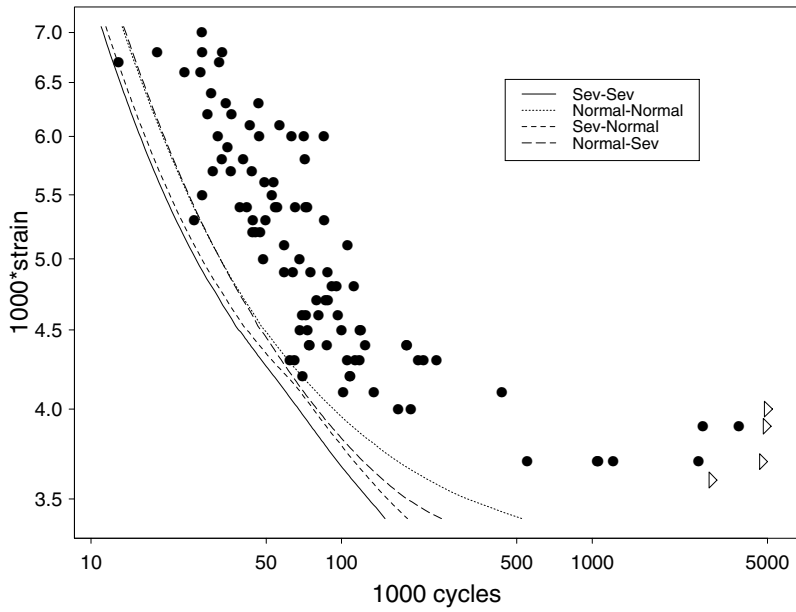


Figure 13: Lower 95% Confidence Lower Bounds for the .05 Quantile of Fatigue Life for the Nickel-Base Superalloy Data

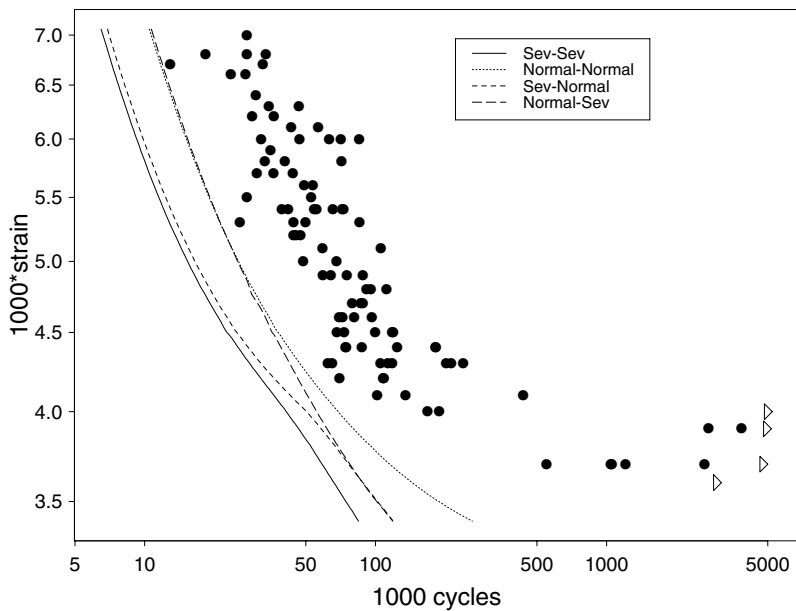


Figure 14: Lower 95% Confidence Lower Bounds for the .01 Quantile of Fatigue Life for the Nickel-Base Superalloy Data

## 5.2 Residual Analysis

Figure 15 gives a plot of the data and the fitted normal-normal model. The plot includes density curves at selected strain levels. Figure 16 gives the corresponding plot of the residuals versus the strain levels. The residual plot does not show any clear patterns in the residuals. The normal-normal model appears to provide an adequate description of the life-strain relationship.

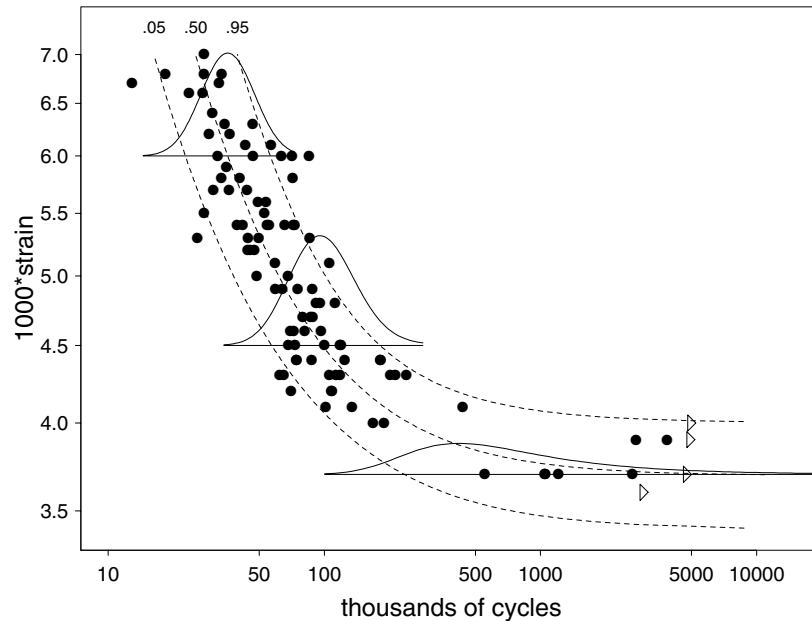


Figure 15: *Log-Log S-N Plot for the Nickel-Base Superalloy Data with ML Estimates of Density Curves and the .05, .50, .95 Quantile Estimates under the Fitted Normal-Normal Model*

## 6 CONCLUSIONS AND AREAS FOR FURTHER RESEARCH

When fatigue limits exist, plots of fatigue life versus stress/strain often exhibit curvature at lower stress/strain levels. Moreover, in most fatigue experiments, the variance of fatigue life decreases as stress/strain increases and the standard deviation is often modeled as a monotonic function of stress/strain. Curvature in the fatigue life versus stress/strain relationship can be modeled by including a constant fatigue-limit parameter in statistical models for fatigue life. Fixed fatigue-limit models, however, do not address the possible variability of the fatigue limit. This variability could be expected to be due to dependence of the fatigue limit on material structural properties that may vary from specimen to specimen. The random fatigue-limit model provides a description of the commonly observed increase in variability in log fatigue life at low levels of stress/strain and suggests a possible physical

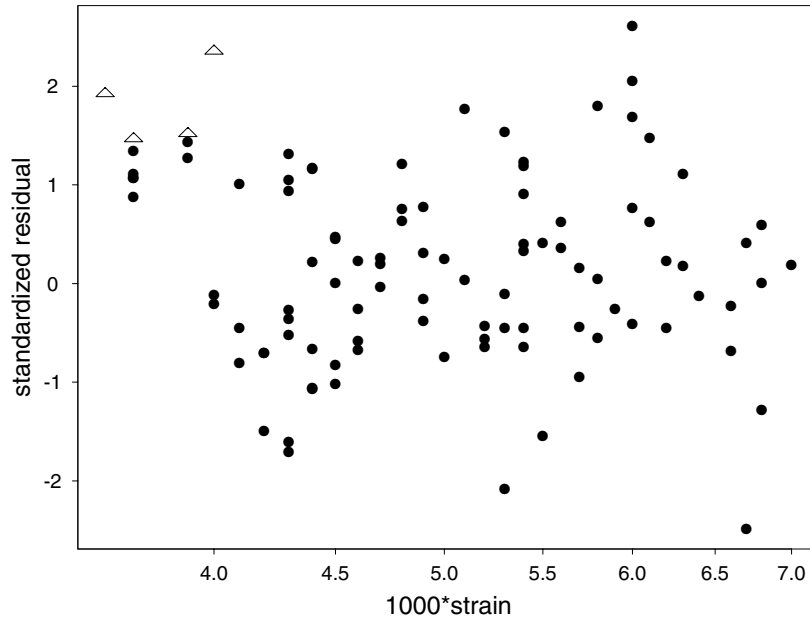


Figure 16: *Plot of Standardized Residuals versus Strain Levels for the Normal-Normal Model Fit to the Nickel-Base Superalloy Data*

explanation for this behavior. These issues are the main motivations for the random fatigue-limit model. The examples considered here show that the random fatigue-limit model is able to address these issues adequately. The model has performed just as well for other datasets relating fatigue life to stress or strain.

Our examples compared the fits of the random fatigue-limit model under different distributional assumptions for both stress and strain fatigue data. In both cases, the normal-normal distribution combination provided the best fit. We compared the ML estimates of the .05, .50, and .95 quantiles and the lower confidence bounds for the .01 and .05 quantiles for different combinations of distributional assumptions. Similar computations and comparisons are possible if the experimenter is interested in other quantities.

There are several of possible extensions that deserve to be explored further:

1. Our examples have used combinations of normal and sev distributions for  $W|V$  and  $V$ . It would be useful to explore the use of other distributions, perhaps motivated from physical theory.
2. It would be useful to combine the analytical approach to testing goodness of fit in Section 4.3 with the P-P plots, giving confidence bands to help one assess the lack of fit of the model distribution. The approach of Nair (1984) could be adapted for this purpose, or corresponding simulation-based methods could be developed.
3. In the preceding examples, we use the AIC statistic to judge which distributional combination of the random fatigue-limit model best approximates the true model.

In both examples, the AIC statistics agree with the information given by Q-Q, P-P, and S-P plots. The AIC may perhaps provide a viable method of comparing different random fatigue-limit models. Linhart (1988) presented a procedure to test whether or not two AIC's differ significantly. The test is based on the asymptotic distribution of the difference between the discrepancies of two AIC's from the true AIC. Using this method instead of simply comparing AIC values provides an objective criterion for comparing competing models.

4. There are important questions about how to design fatigue experiments under the random fatigue-limit model. Traditional methods will have to be extended to account for the nonlinear relationship between life and stress. Large-sample approximations would provide easy-to-compare evaluations of test plan properties with respect to the efficiency of estimating quantities of interest. Simulation studies require much more computer time but can be conducted to study the small-sample properties of the test plans. This is currently under investigation.

## Acknowledgments

We thank Wayne Nelson for suggesting the problem to us and making helpful suggestions on an earlier version of this article and Paul Wirsching of the University of Arizona for providing datasets and important references. Thanks to the editor, associate editor and referees for valuable comments and suggestions. Computing for the research reported in this article was run using the equipment in the Department of Statistics, purchased with funds provided by an National Science Foundation SCREMS grant award DMS 9707740 to Iowa State University.

## REFERENCES

- Akaike, H. (1973), "Information Theory and an Extension of the Maximum Likelihood Principle." in *2nd International Symposium on Information Theory*, Budapest: Akademiai Kiado, pp. 267-281.
- Colangelo, V. J. and Heiser F. A. (1974), *Analysis of Metallurgical Failures*, New York: Wiley.
- Collins, J. A. (1993), *Failure of Materials in Mechanical Design*, New York: Wiley.
- Crowder, M., Kimber, A., Smith, R., and Sweeting, T. (1991), *Statistical Analysis of Reliability Data*, London: Chapman & Hall.
- D'Agostino, R., and Stephens, M. (1986), *Goodness-of-Fit Techniques*, New York: Marcel Dekker.
- Dieter, G. E. (1976), *Mechanical Metallurgy*, New York: McGraw-Hill.
- Hirose, H. (1993), "Estimation of Threshold Stress in Accelerated Life-Testing," *IEEE Transactions on Reliability*, 42, 650-657.

- Klesnil, M., and Lukáš, P. (1992), *Fatigue of Metallic Materials*, New York: Elsevier.
- Little, R. E. (1974), "The Up-and-Down Method for Small Sample With Extreme Value Response Distributions," *Journal of the American Statistical Association*, 69, 803-806.
- Little, R. E. (1990), "Optimal Stress Amplitude Selection in Estimating Median Fatigue Limits Using Small Samples," *Journal of Testing and Evaluation*, 18, 115-122.
- Michael, J. R. (1983), "The Stabilized Probability Plot," *Biometrika*, 70, 11-17.
- Nair, V. N. (1984), "Confidence Bands for Survival Functions With Censored Data: A Comparative Study," *Technometrics*, 26, 265-275.
- Nelson, W. (1973), "Analysis of Residuals From Censored Data," *Technometrics*, 15, 697-715.
- Nelson, W. (1984), "Fitting of Fatigue Curves With Nonconstant Standard Deviation to Data with Runouts," *Journal of Testing and Evaluation*, 12, 69-77.
- Nelson, W. (1990), *Accelerated Testing: Statistical Models, Test Plans, and Data Analyses*, New York: Wiley.
- Ostrouchov, G., and Meeker, W. Q. (1988), "Accuracy of Approximate Confidence Bounds Computed From Interval Censored Weibull and Lognormal Data," *Journal of Statistical Computing and Simulations*, 29, 43-76.
- Pascual, F. G., and Meeker, W. Q. (1997), "Analysis of Fatigue Data with Runouts Based on a Model with Nonconstant Standard Deviation and a Fatigue Limit Parameter," *Journal of Testing and Evaluation*, 25, 292-301.
- Ross, J. S. (1990), *Nonlinear Estimation*, New York: Springer-Verlag.
- Shen, C. L. (1994), "Statistical Analysis of Fatigue Data," unpublished Ph.D. dissertation, University of Arizona, Department of Aerospace and Mechanical Engineering.
- Shen, C. L., Wirsching, P. H., and Cashman, G. T. (1996a), "An Advanced Comprehensive Model for the Statistical Analysis of S-N Fatigue Data," unpublished manuscript, University of Arizona, Department of Aerospace and Mechanical Engineering.
- Shen, C. L., Wirsching, P. H., and Cashman, G. T. (1996b), "Design Curve to Characterize Fatigue Strength," *Journal of Engineering Materials and Technology*, 118, 535-541.
- Shimokawa, T., and Hamaguchi, Y. (1987), "Statistical Evaluation of Fatigue Life and Fatigue Strength in Circular-Holed Notched Specimens of a Carbon Eight-Harness-Satin/Epoxy Laminate," in *Statistical Research on Fatigue and Fracture (Current Japanese Materials Research, Vol. 2)*, eds. T. Tanaka, S. Nishijima, and M. Ichikawa, London: Elsevier, pp. 159-176.
- Symonds, J. (1996), "Mechanical Properties of Materials" in *Marks' Standard Handbook for Mechanical Engineers*, eds. E. A. Avallone and T. Baumeister III, New York: McGraw-Hill, Chapter 5, pp. 2-15.

Vander Wiel, S. A., and Meeker, W. Q. (1990), "Accuracy of Approximate Confidence Bounds Using Censored Weibull Regression Data From Accelerated Life Tests," *IEEE Transactions on Reliability*, R-39, 346-351.

Wilk, M. B., and Gnanadesikan, R. (1968), "Probability Plotting Methods for the Analysis of Data," *Biometrika*, 55, 1-19.